International Conference
Nuclear Energy in Central Europe 2001
Hoteli Bernardin, Portorož, Slovenia, September 10-13, 2001
www: http://www.drustvo-js.si/port2001/ e-mail: PORT2001@ijs.si
tel.:+ 386 1 588 5247, + 386 1 588 5311 fax:+ 386 1 561 2335
Nuclear Society of Slovenia, PORT2001, Jamova 39, SI-1000 Ljubljana, Slovenia

ADVANCED MODELLING AND NUMERICAL STRATEGIES IN NUCLEAR THERMAL-HYDRAULICS

Herbert Städtke
Commission of the European Communities
Joint Research Centre – Ispra Establishment
I-21020 Ispra, (Varese) Italy
e-mail: herbert.staedtke@jrc.it

ABSTRACT

The first part of the lecture gives a brief review of the current status of nuclear thermal hydraulics as it forms the basis of established system codes like TRAC, RELAP5, CATHARE or ATHLET. Specific emphasis is given to the capabilities and limitations of the underlying physical modelling and numerical solution strategies with regard to the description of complex transient two-phase flow and heat transfer conditions as expected to occur in PWR reactors during off-normal and accident conditions.

The second part of the lecture focuses on new challenges and future needs in nuclear thermal-hydraulics which might arise with regard to re-licensing of old plants using best-estimate methodologies or the design and safety analysis of Advanced Light Water Reactors relying largely on passive safety systems. In order to meet these new requirements various advanced modelling and numerical techniques will be discussed including extended well-posed (hyperbolic) two-fluid models, explicit modelling of interfacial area transport or higher order numerical schemes allowing a high resolution of local multi-dimensional flow processes.

1 INTRODUCTION

There is arguably no other field of engineering, which depends so strongly on "numerical process simulation" as nuclear technology and especially nuclear safety. This is mainly due to two major reasons (1) the impracticality of executing full-scale safety related experiments and (2) the absence of simplified scaling laws for the governing processes which would allow a direct transfer of results from small scale test facilities to the full size plant.

Previous attempts in reactor safety analysis including the definition of a limited number of worst-case scenarios in combination with conservative modelling assumptions have been replaced by "best-estimate" methodologies. The best-estimate approach aims to provide a detailed realistic description of postulated accident scenarios based on best-available modelling methodologies and numerical solution strategies which have been sufficiently verified against experimental data from differently scaled separate effects and integral test facilities.

It is evident that each model or code represents an approximation of the real system or plant. The final use of these codes will therefore largely depend on the progress in quantifying the uncertainty associated with the prediction of the plant behaviour which will be addressed in a separate report.

2 CURRENT STATUS OF NUCLEAR THERMAL-HYDRAULICS

2.1 Common Physical Modelling Basis

The most challenging task for the thermal-hydraulic codes is related to the modelling of transient two-phase flow processes including boiling and condensation heat transfer. Nearly all current two-phase flow models used in present "best estimate" thermal hydraulic codes are based on "average" flow parameters rather than local flow quantities. The corresponding "macroscopic" separate balance equations for the two phases are obtained by a space and/or time (or ensemble) averaging of the local instantaneous phasic flow equations. This leads to what is often referred to as the "two-fluid model" of two-phase flow where both phases are treated as interpenetrating continua with source terms representing the interfacial transport processes for mass, momentum and energy. As is the case for all such averaging processes, information on local flow processes, in particular at the interface separating the two phases or at the region near the walls, is lost and has to be compensated by additional modelling. The development of such two fluid models is largely attributable to the work of Ishii [1], Boure [2], Delhaye and Achard [3] and Drew and Lahey [4].

2.2 Basic Flow Equations of Two-Fluid Model

As the result of the space/time averaging of the instantaneous phase equations, the "macroscopic" balance equations of the single pressure two-fluid model can be formulated for vapour $(i = g)$ and liquid $(i = l)$ as

mass:

$$\frac{\partial}{\partial t}(\alpha_i \rho_i) + \nabla \cdot (\alpha_i \rho_i \vec{v}_i) = \Gamma_i \tag{1}$$

with $\sum_{i=g,l} \Gamma_i = 0$

momentum:

$$\frac{\partial}{\partial t}(\alpha_i \rho_i \vec{v}_i) + \nabla \cdot (\alpha_i \rho_i \vec{v}_i \vec{v}_i) + \alpha_i \nabla p + (p^{\text{int}} - p)\nabla \alpha_i - \nabla \cdot \left(\alpha_i \overline{\overline{\mathbf{T}}}\right) = \vec{F}_i^{\text{int}} + \Gamma_i \vec{v}_i^{\text{int}} + F_i^{ext} \tag{2}$$

with $\sum_{i=g,l} \vec{F}_i^{\text{int}} = 0$

energy:

$$\frac{\partial}{\partial t}\left[\alpha_i \rho_i \left(u_i + \tfrac{1}{2}\vec{v}_i^{\,2}\right)\right] + \nabla \cdot \left[\alpha_i \rho \vec{v}_i \left(h_i + \tfrac{1}{2}\vec{v}_i^{\,2}\right)\right] + p^{\text{int}} \frac{\partial \alpha_i}{\partial t} - \nabla \cdot \left(\alpha_i \overline{\overline{\mathbf{T}}}_i \cdot \vec{v}_i\right) = Q_i^{\text{int}} + \Gamma_i \left(h_i + \tfrac{1}{2}v_i^2\right)^{\text{int}} + \vec{F}_i^{\text{int}} \cdot \vec{v}^{\text{int}} + F_i^{ext} \cdot \vec{v}_i + Q_i^{ext} \tag{3}$$

with $\sum_{i=g,l} \left[Q_i + \Gamma_i \left(h_i + \tfrac{1}{2}v_i^2\right)\right]^{\text{int}} = 0$

In most TH-codes the primary and secondary systems are modelled as a coupled thermal-hydraulic network using one-dimensional components. The separated 1-D balance

equations can be written for quasi one-dimensional flow in pipes with varying cross section $A(x)$as:

mass:

$$\frac{\partial}{\partial t}(\alpha_i \rho_i) + \frac{1}{A}\frac{\partial}{\partial x}(\alpha_i \rho_i \vec{v}_i A) = \Gamma_i \tag{4}$$

momentum:

$$\begin{aligned} &\frac{\partial}{\partial t}(\alpha_i \rho_i \upsilon_i) + \frac{1}{A}\frac{\partial}{\partial x}(\alpha_i \rho_i \upsilon_i^2 A) + \alpha_i \frac{\partial p}{\partial x} + \Delta p^{\text{int}} \frac{\partial \alpha_i}{\partial x} = \alpha_i \rho_i F^{ext} \\ &+ \alpha_i \rho_i F_i^{wal} + \alpha_i \rho_i F_i^{\text{int}} + \Gamma_i (\upsilon^{\text{int}} - \upsilon_i) + F_i^{vir} \end{aligned} \tag{5}$$

energy:

$$\begin{aligned} &\frac{\partial}{\partial t}\left[\alpha_i \rho_i (u_i + \upsilon_i^2)\right] + \frac{1}{A}\frac{\partial}{\partial t}\left[\alpha_i \rho_i \upsilon_i (h_i + \upsilon_i^2) A\right] + \alpha_i \frac{\partial p}{\partial t} = Q_i^{\text{int}} + Q_i^{wall} \\ &+ \Gamma_i \left(h_i + \tfrac{1}{2}\upsilon_i^2\right)^{\text{int}} + {}_i\, F_i^{ext} + F_i^{wal} \upsilon_i^2 + F_i^{\text{int}} \upsilon_i \end{aligned} \tag{6}$$

Due to the pressure coupling terms, the separated momentum at energy equations can not be put into a fully conservative form which might have some consequences for their numerical integration.

2.3 Closure Laws

The system of balance equations (1) to (3) or (4) to (6) respectively has to be completed by constitutive relations for the source terms on the right-hand side of the equations which can be grouped into four categories:

2.3.1 External Momentum and Energy Sources

For external body forces normally only gravity is of interest with $F_i^{ext} = \alpha_i \rho_i g$. As external energy sources Q_i^{ext} the instantaneous fission power and the power related to the decay of fission products have to be considered which are calculated by neutron kinetics models. Normally point kinetics models are applied in most TH-codes which might be adequate for many transient and accident conditions.

2.3.2 Non-viscous Interfacial Forces

Interfacial forces are usually split into a viscous part (interfacial drag) and non- viscous part (virtual or added mass term) $F_i^{\text{int}} = F_i^{drag} + F_i^{vir}$. The virtual mass forces result from the coupling with the surrounded fluid in the case of relative acceleration of a particle (bubble or droplet). Apart from ideal flow conditions (e.g. potential flow around spheres), there is no way to derive the formulations for the virtual mass effects from basic principles. Several, slightly different forms of this term can be found in the literature which are often not free of some heuristic elements. A rather general formulation has been derived by Drew and Lahey [5] based in the objectivity principle (invariant on coordinate system transformation) which can be written as:

$$F_g^{vm} = -F_l^{vm}$$
$$= C^{vm}\alpha_g\alpha_l\rho_m\left[\left(\frac{\partial v_g}{\partial t}+v_l\frac{\partial v_g}{\partial x}\right)-\left(\frac{\partial v_l}{\partial t}+v_g\frac{\partial v_l}{\partial x}\right)-(1-\lambda)(v_g-v_l)\frac{\partial}{\partial x}(v_g-v_l)\right] \quad (7)$$

with the mixture density $\rho_m = \alpha_g\rho_g + \alpha_l\rho_l$. For the open parameter λ different values are used in the codes, e.g. $\lambda = 1$ in earlier versions of the REPAP5 code (Mod1/Mod2), or $\lambda = 2$ in CATHARE.

The virtual mass coefficient in (7) is normally bounded between $0.0 \le C^{vm} \le 1.0$. In some cases a flow regime dependent value is used, e.g. $C^{vm} = 0.5$ for dispersed bubbly or droplet flow or $C^{vm} = 0.0$ for fully separated phases like stratified flow conditions.

2.3.3 Source Terms Describing Interfacial Transport Processes

The sources describing the interfacial mass, momentum and energy exchange processes between the phases, $S_i^{\text{int}} = \Gamma_i$, F_i^{int}, Q_i^{int}, are assumed to be algebraic functions of the form

$$S_i^{\text{int}} = C_i^{\text{int}} a^{\text{int}} X_i \quad (8)$$

with the interfacial area concentration (interfacial area per unit volume) a^{int}, a driving force (in the sense of non-equilibrium thermodynamics) X_i, and a corresponding transfer parameter C_i^{int}. The driving forces X_i are assumed to be linear (or higher order) functions of parameters describing the deviations from the thermal and mechanical equilibrium between the phases: e.g. superheating of the gas and liquid phase, $T_g - T_{sat}$, and $T_l - T_{sat}$, respectively, for the heat and mass transfer processes and the "slip" velocity, $v_g - v_l$, for interfacial friction (drag). The interfacial transfer coefficients C_i^{int} for interfacial drag, interfacial heat and mass transfer are calculated from local flow parameters using flow regime dependent empirical correlations or simplified mechanistic models.

As indicated in equation (8) a key parameter for the interfacial transfer process is the *interfacial area concentration* which depends strongly on the (local) spatial phase distribution as characterized by the two-phase flow regime. Since the balance equations (1) to (3) or (5) to (7) give no information on the two-phase flow structure, additional modelling is required to provide an (at least) approximate value for the interfacial area concentration.

The standard approach in nearly all TH-codes is to correlate the interfacial area concentration with known, major governing state and transport parameters like volumetric concentration of vapour and liquid, α_g and α_l, phase velocities, densities, viscosity, or surface tension. This is usually done via *flow regime maps* which identify a specific two-phase structure on the basis of measured or predicted flow parameters. Criteria for the flow regime boundaries are either completely empirical or are derived from Kelvin-Helmholtz or Rayleigh-Taylor instability criteria. Specifically modelled are bubbly, slug, annular-mist, mist and stratified flow regimes. More complex or less well-structured flow regimes and flow regime transitions are dealt with by purely mathematical interpolation procedures using linear or higher order interpolation functions.

Strictly speaking, all these flow regime maps are valid only for steady state and fully developed flow conditions which normally do not exist in nuclear reactors under transient or accident conditions.

2.3.4 Wall heat transfer

The energy transfer between the fluid and solid structure (fuel rods, SG U-tubes, pipe and vessel walls) includes two coupled processes, the transient (non-stationary) heat conduction in the solid structure and the heat transfer processes at the wall surface adjacent to the fluid. The total wall heat transfer includes the wall-to-liquid and wall to-vapour contributions

$$Q^{tot} = \frac{1}{d}\left[H_l^w\left(T^w - T_l\right) + H_g^w\left(T^w - T_g\right)\right] \tag{9}$$

with the wetted perimeter d (wetted wall surface per unit volume), wall temperature T^w, the bulk phasic temperatures T_l and T_g, and the wall heat transfer coefficients for liquid and vapour H_l^w and H_g^w.

For the wall-to-liquid and wall-to-gas heat transfer coefficients, highly empirical correlations are usually used dependent on the prevailing heat transfer regime. The heat transfer regimes normally modelled include: (1) forced convection to single-phase liquid, (2) nucleate boiling, (3) transition boiling, (4) film boiling, (5) convection to single-phase vapour, (6) convection to two-phase mixture, (7) natural convection to single-phase liquid.

Additional correlations are used for the critical heat flux which establishes the boundary between nucleate and transition boiling, and the minimum stable film boiling temperature which provides the boundary between transition and film boiling. A heat transfer selection logic is normally used which identifies the individual heat transfer regime on the basis of local flow parameters and wall surface temperature.

2.4 Final Comments to the Two-Fluid Model

In many cases the two-fluid model outlined above represents only a rough approximation to the real flow situation. This might be already the case for rather well structured flow regimes like bubbly flow with a continuous distribution of bubble sizes. It is obvious that lumping together all the bubbles into one pseudo-fluid cannot describe the size-dependent behaviour of individual bubbles (or classes of bubbles) and the associated dispersion of the gas phase. Similar considerations might be valid for dispersed droplet or mist flow The situation becomes even more critical in the case of less structured or more complex flow regimes like annular mist and inverted annular flow where multi-fluid models might be more appropriated.

As outlined above, the modelling of the interfacial laws represents the weakest point in the two-fluid approach to describe transient two-phase flow and no significant progress has been made in this area over the last ten years. The major problem comes from the fact that, up to now, there is no way to directly measure the interfacial transport processes. A considerable improvement might be expected from an explicit modelling of the interfacial area transport as will be outlined below, however, this will be strongly related to the success in development of appropriate measurement techniques for their verification.

The resulting system of equations is (in most cases) characterized by complex conjugate eigenvalues even in the case when all viscosity or diffusion terms are dropped. This indicates that the model represents an ill-posed initial/boundary value problem which has been extensively (and controversially) discussed in the past with respect to the prediction accuracy and numerical stability [6]. However, experience in applying these models has shown that in most applications stable solutions can be obtained since the present numerical techniques used in all the codes provide a sufficiently large damping mechanism but at the expense of large artificial diffusion or viscosity effects. In some cases, additional time and space derivative

terms have been included in the two separated momentum equations to account for additional (non-viscous) forces resulting from virtual or added mass effects which makes the two-fluid model hyperbolic. However, the effect of these terms has always been rendered negligible due to the overwhelming damping and artificial diffusion effects of the numerical method presently used in the codes.

3 NUMERICAL METHODS AS USED IN THERMAL-HYDRAULIC SYSTEM CODES

3.1 Spatial discretization

All of the presently well-established codes are using finite difference, first-order numerical methods based on staggered grid and donor cell techniques as schematically shown for 1-D flow conditions in Fig.1.

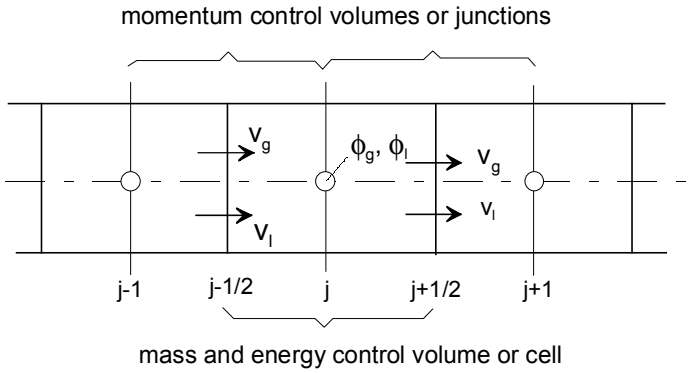

Figure 1: Space discretization for one-dimensional flow

To evaluate the mass and energy balances for the computational cells or volumes the corresponding fluxes at the cell interfaces (junctions) are needed which involve beside the phasic velocities also the void fraction and phasic densities and internal energies. These scalar variables ϕ are taken from the upstream or donor cell as

$$\dot{\phi}_{j+1/2} = \frac{1}{2}\left[(\phi_i)_j + (\phi_i)_{j+1}\right] + \frac{1}{2}\frac{v_i}{|v_i|}\left[(\phi_i)_j - (\phi_i)_{j+1}\right] \quad \text{with} \quad \phi_i = \alpha_i, \rho_i, u_i \tag{10}$$

From equation (10) it is evident that discontinuities will appear in the junction scalar parameters in case of flow reversal. A further inconsistency might arise in case of counter-current flow where a void fraction is calculated which is inconsistent with the condition $\alpha_g + \alpha_l = 1$.

Although the staggered grid/donor method is known to introduce a substantial amount of numerical (artificial) diffusion or viscosity, it is preferred due to the inherent numerical stability. This is of specific importance since most codes are using two-fluid models having complex characteristics which suffer from small wave-length (high frequency) instabilities.

3.2 Time Integration

Apart from the staggered grid and donor cell approach, the numerical methods largely differ in the degree of implicitness for the time integration. The NRC sponsored codes RELAP5 [7] and TRAC [8] are using an extension of the Implicit Continuous Eulerian ICE method originally developed for the solution of single-phase gas dynamics problems [9] and later

extended also for transient two-phase flow conditions [10]. The ICE technique is expected to provide stable results for time step sizes below the material Courant limit, however applying the method for two-phase flow predictions often shows a rather high level of numerically induced (unphysical) oscillations. A further problem of the ICE technique is that it does not *a priori* guarantee the conservation of mass and energy.

In RELAP5, a one-step, semi-implicit method is applied where the whole system is reduced to the direct solution for the new-time pressure values (without any iteration). All other parameters are then calculated by back-substitutions. The appearing mass error is used as a parameter for the time step control.

The TRAC code uses a Stability Enhancing Two-Step (SETS) method [11,12], where the semi-implicit step is used only as an intermediate result, followed by a "stabilizer step" to provide conservation of mass and energy for the two separated phases.

Of large importance in the numerical approach is the way the interfacial transport processes are dealt with which might be characterized by rather small time constants. In RELAP5 and TRAC the related source terms are treated only in a partially implicit manner (e.g. using new time values for phasic velocities or temperature) which might result in numerical instabilities. For this reason additional damping procedures like an "under-relaxation" are often applied (as in RELAP5) where the related source terms are weighted between the old and the new time values.

The above mentioned problems with respect to time step limitations and/or numerical stability can be largely avoided if fully implicit time integration techniques are used as in CATHARE [13] and ATHLET [14]. However, the principal advantage of fully implicit methods might be compromised by the large numerical effort needed for the matrix inversion, in particular for large (3-dimensional) systems. For this purpose a partially implicit "two-step" numerical scheme similar the SETS method is used in the CATHARE code for the 3-dimensional reactor pressure vessel module.

3.3 Nodalization Schemes and Multi-dimensional Effects

In most cases rather coarse nodalization diagrams are applied where even complex reactor systems are represented by a relatively small number of nodes, often in the range of 300 to 500. From this it is clear that important local phenomena can not always be described. Only few attempts have been made to systematically investigate the effects of the nodalization or the convergence of the predicted results in case of a continuous increase of the number of computational cells or control volumes. Such studies have always been hampered by several reasons including economic constraints and stability problems particularly in case of small cell sizes.

Another problem is related to the modelling of multi-dimensional effects which are always present in the full-size plant as well as in scaled integral test facilities. The strictly one-dimensional codes like RELAP5 or ATHLET try to handle this situation by multiple junction connections to a (one-dimensional) computational cell or by using a parallel channel representation with cross junction connections). The results obtained are very sensitive to the chosen nodalization details, and other input parameters like flow resistance and form loss coefficients. Since no general guidelines exist, a large degree of freedom is left to the code user to make best use of the various possibilities for his specific problem.

Explicit 3-dimensional modules exist as an option in the codes TRAC and CATHARE for the reactor pressure vessel. They represent a straightforward extension of the one-dimensional modules for cylindrical coordinates. Due to the heavy computational effort needed, the 3-dimensional modules are used only for fast (short) transients like large break LOCA. In most applications, extremely coarse nodalization schemes are applied and

consequently the advantage of a 3-dimensioanl modelling of the flow processes might be largelycompromised. As for all attempts to simulate 3-dimensional two-phase flow processes, the modules suffer from the large numerical (artificial) diffusion/viscosity effects and the lack of appropriate bulk (physical) diffusion and turbulence models. To a certain extent both shortcomings might compensate each other in a non-physical manner.

4 FUTURE NEEDS AND CHALLENGES IN NUCLEAR THERMAL-HYDRAULICS

The basic thermal hydraulic models and numerical methods used in present TH-system codes are largely based on the extensive research efforts spent in the past, mainly in the sixties and seventies and no longer reflect present state-of-the-art in two-phase flow modelling or computational fluid dynamics.

Although the codes demonstrated stable and reliable results for many accident scenarios they might not be adequate for future needs. Such future challenges might arise from

- Re-licensing of older plants with regard to power-upgrading or life-time extension using best-estimate licensing procedures
- Design and safety analysis of Advanced Light Water Reactors (ALWR) or Generation IV reactors relying largely on passive safety systems characterized by low pressure low flow transients, two-phase natural convection or strong coupling of the behaviour in primary coolant system and containments.
- Limited availability of experimental data bases due to the closure of expensive test facilities.

The fulfillment of needs will require the development of a new generation of codes based on a more generic two-phase flow modelling and an improved 3-dimensional prediction capability using advanced numerical concepts. Some possible features of such TH-code will be discussed in the next section.

5 ADVANCED MODELLING AND NUMERICAL SOLUTIONS STRATEGIES

At the JRC Ispra, a research project was started about 10 years ago to explore some promising advanced modelling and numerical concepts which might have the potential overcome limitations and deficiencies of current TH-codes as described above. Major emphasis in the activity is given to numerical simulation of multi-dimensional two-phase flows based on extended multi-fluid (hyperbolic) models. A consequence of this activity has been the development and use of extended systems of improved (hyperbolic) two fluid models and the application of low diffusive, state-of-the-art numerical techniques which make explicit use of the hyperbolic nature of the flow equations.

The project forms part of the EU funded Advanced Three-dimensional Two-phase Flow Simulation Tool for Application to Reactor Safety (ASTAR) project, a Shared Cost Action partially funded by the EU within the 5th Framework Programme on Community Research in the Area of Nuclear Fission. A major aim of the project is to combine and harmonize various attempts in the development of 3-D transient two-phase flow as a basis for a new generation of thermal hydraulic codes [15].

5.1 Physical Models

5.1.1 Hyperbolic Two-phase flow model

The heart of the development has been a new hypberbolic model for inhomogeneous, non-equilibrium two-phase flow for the whole range of void fraction from single-phase liquid to vapour. The hyperbolicity condition has been achieved by an appropriate formulation of "non-viscous" interfacial forces. As a result of a comprehensive study the following form has been derived [16]

$$\vec{F}_i^{vm} = -\alpha_g \alpha_l \rho C^{vm} \left(\frac{d\vec{v}_g}{dt} - \frac{d\vec{v}_l}{dt} \right) + \alpha_g \alpha_l \left(\alpha_g \rho_l - \alpha_l \rho_g \right) \left[\left(\vec{v}_g - \vec{v}_l \right) \Delta \cdot \left(\vec{v}_g - \vec{v}_l \right) \right]$$
$$- \alpha_g \alpha_l \left(\rho_g + \rho_l \right) \left(\vec{v}_g - \vec{v}_l \right) \cdot \alpha_g - \alpha_g \alpha_l \left(\rho_g + \rho_l \right) \left(\vec{v}_g - \vec{v}_l \right) \left(\frac{\alpha_g}{\rho_g} \frac{d\rho_g}{dt} + \frac{\alpha_l}{\rho_l} \frac{d\rho_l}{dt} \right) \tag{11}$$

with the total derivative terms

$$\frac{d^j \vec{v}_i}{dt} = \frac{\partial \vec{v}_i}{\partial t} + \left(\vec{v}_j \cdot \Delta \right) \vec{v}_i . \tag{12}$$

Introducing this formulation into the system of governing equations, here written in a compact matrix form,

$$\frac{\partial \boldsymbol{U}}{\partial t} + \vec{\boldsymbol{G}}_{adv} \cdot \left(\nabla \boldsymbol{U} \right) = \boldsymbol{S} \tag{13}$$

all eigenvalues of the coefficient matrix $\vec{\boldsymbol{G}}_{adv}$ are real and a set of independent eigenvectors is obtained. A specific feature of the model is that both eigenvalues and eigenvectors can be expressed as algebraic functions of the governing flow parameters. The various eigenvalues can be identified as the following characteristic velocities in the ζ - direction (see Fig. 2).

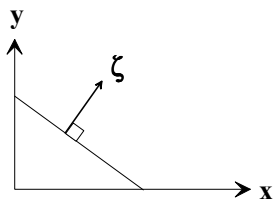

$\lambda_{1,2} = \vec{v}_g \cdot \vec{n}_\zeta ,\ \vec{v}_f \cdot \vec{n}_\zeta$		void waves
$\lambda_{3,4} = \vec{v} \cdot \vec{n}_\zeta + a$		pressure/densitywaves
$\lambda_{5,6} = \vec{v}_g \cdot \vec{n}_\zeta ,\ \vec{v}_f \cdot \vec{n}_\zeta$		shear waves
$\lambda_{7,8} = \vec{v}_g \cdot \vec{n}_\zeta ,\ \vec{v}_f \cdot \vec{n}_\zeta$		temperature/entropy waves
$\lambda_9 = \vec{v}^{\,\mathrm{int}} \cdot \vec{n}_\zeta$		interfacial area waves

Figure 2: Direction of wave propagation and characteristic wave speeds

with the phase velocities, $\vec{v}_g$ and $\vec{v}_f$, the mixture flow velocity $\vec{v}$ and sound velocity a. More detailed information on the various wave propagation mechanisms can be obtained from the corresponding eigenvectors as explained in more detail in [16,17].

The algebraic formulation of the eigenvalues and the corresponding set of eigenvectors. allow a decomposition of the coefficient matrix $\vec{\mathbf{G}}$ with respect to individual characteristic velocities in a purely algebraic way which is of large advantage for a class of advanced numerical techniques described below.

5.1.2 Interfacial Area Concentration

An alternative to the static correlation of the interfacial area based on flow regime maps is the explicit dynamic modelling of the transport of interfacial area as is discussed in some detail by Kocamustafaogullari and Ishii [18].

Basically, the interfacial area transport model consists of a balance equation for interfacial area concentration

$$\frac{\partial}{\partial t}\left(a^{\text{int}}\right)+\nabla\cdot\left(a^{\text{int}}\vec{v}^{\text{int}}\right)=\sigma^{A}+C^{\text{int}}\left[\frac{\partial}{\partial t}\alpha_{g}+\Delta\cdot\left(\alpha_{g}\vec{v}^{\text{int}}\right)\right] \tag{14}$$

The source terms on the right side of equation (14) account for the production and destruction of interfacial area at constant void fraction due to flow regime transitions or processes like particle (droplet or bubble) deformation, break-up or coalescence, σ^{A}, and the interfacial area changes linked with the changes of void fraction due to depressurization or mass change (evaporation/condensation).

The interfacial area transport model is very attractive since it allows the description of interfacial processes as a dynamic, time-dependent process and is expected also to provide a more physically-based prediction of flow regime transitions. However, as is true for all time and space averaged approaches, the crucial point is always the formulation of the corresponding source or sink terms σ^{A} and the interfacial velocity v^{int} which is discussed further in [18]. So far, interfacial area transport models have been applied only to rather well-structured flow regimes like mono-dispersed bubbly or droplet flows (see for example in Staedtke *at al* [19]). To extend the approach to more complex flow regimes and for regime transition processes will require more research work and possibly also new instrumentation and measurement techniques for their verification and validation.

5.2 Numerical Method

Within the last two decades much progress has been made in the development of high order numerical schemes for single-phase gas dynamics calculational methods allowing a high resolution of local flow phenomena and discontinuities. They include for example the Split Coefficient Matrix method, the Flux Vector Splitting technique or the method based on the Approximate Riemann Solver.

Common to all these methods is the concept of “upwinding” which combines the preservation of signal propagation processes along characteristic directions with the conservation property for mass, momentum and energy, for the solution of the advection problem. Furthermore, what makes these methods attractive is the fact that they are principally based on a “true” finite volume concept which allows a straightforward application also for unstructured grids. Application of the methods described above for two-phase flow processes has been largely hampered by the requirement for hyperbolicity of the governing system of equations which is not *a priori* the case for the two-fluid model.

5.2.1 Finite Volume Approximation

For the numerical solution, the governing equations are transformed into the conservative form

$$\frac{\partial \boldsymbol{V}}{\partial t}+\nabla\cdot\boldsymbol{F}+\boldsymbol{H}^{nc}\nabla\cdot\boldsymbol{V}=\boldsymbol{S} \tag{15}$$

with the state vector of conservative variables, ***V,*** the corresponding flux vector, ***F*** and the source vector, ***S,*** which includes the volume source terms for mass, momentum, energy and interfacial area.

The "non-conservative" part of the coefficient matrix, $\boldsymbol{H}^{nc}$, in equation (15) reflects the fact that the separate momentum and energy equations cannot be put into a fully conservative form due to some coupling terms including time and space derivative terms.

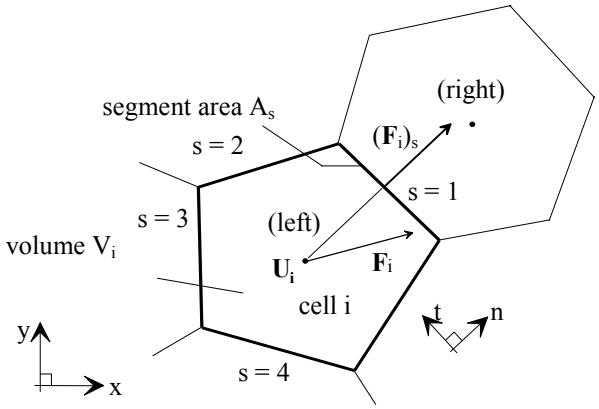

Figure 3: Finite volume discretization

For the numerical solution scheme, the governing equations (15) are transformed into a finite volume approximation for arbitrary polygon-based (2-D) or tetrahedron-based (3-D) unstructured meshes (Fig. 2), as given by

$$\boldsymbol{V}_i^{n+1} = \boldsymbol{V}_i^n - \frac{\Delta t}{V_i}^{n+1} \sum_s A_s \left(\hat{\boldsymbol{F}}_i\right)_s^{n+1} - \frac{\Delta t}{V_i} \sum_s A_s \left(\boldsymbol{H}_i^{nc}\right)_s^{n+1} \left(\hat{\boldsymbol{F}}_i\right)_s^{n+1} + \boldsymbol{S}_i^{n+1} \Delta t \tag{16}$$

with the new and old-time vector of conserved variables, $\boldsymbol{V}_i^{N+1}$ and $\boldsymbol{V}_i^N$, the numerical fluxes $\left(\hat{\boldsymbol{F}}_i\right)_s = \vec{\boldsymbol{F}}_i \cdot \vec{n}_s$ at the interface between the computational cells and the source term vector $\boldsymbol{S}_i^{n+1}$.

5.2.2 Flux Vector Splitting Technique

The numerical fluxes $\boldsymbol{F}_i$ are calculated from a series of linearized quasi-one-dimensional Riemann Problems normal to the specific surface areas of the computational cell boundary segments, as shown schematically in Fig. 4. This yields the "Godunov" fluxes at the cell interface, $\hat{\boldsymbol{F}}_s$,

$$\hat{\boldsymbol{F}}_s = \sum_{k,\lambda_k \geq 0} [\boldsymbol{R}_s] \boldsymbol{F}_l + \sum_{k,\lambda_k \leq 0} [\boldsymbol{R}_s] \boldsymbol{F}_r \tag{17}$$

where the "weighting" factors for the left and right fluxes in equation (17) are the sums of the split coefficient matrices for fluxes ordered with respect to the sign of the corresponding eigenvalue λ_k.

A nearly second-order accuracy is obtained by a linear re-construction of the solution in all computational cells following the Monotonic Upwind Scheme for Conservation Laws (MUSCL) approach of Van Leer [20].

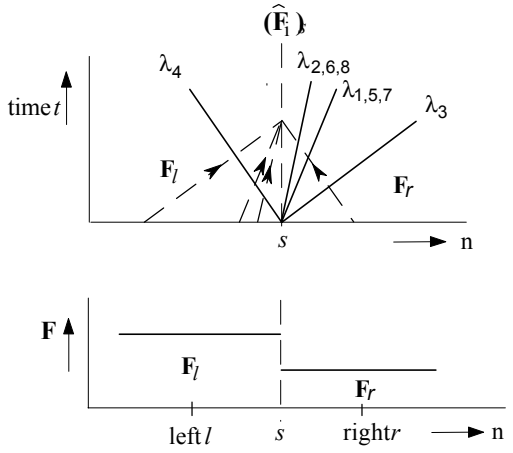

Figure 4: Linearized Riemann problem for two-phase flow

5.2.3 Implicit Time Integration

For the *implicit time integration*, both the source terms and the fluxes are evaluated by a first-order Taylor expansion up to the new-time step values

$$\boldsymbol{S}_i^{n+1} = \boldsymbol{S}_i^n + \left(\frac{\partial \boldsymbol{S}}{\partial \boldsymbol{U}}\right)_i^n \left(\boldsymbol{U}_i^{n+1} - \boldsymbol{U}_i^n\right), \qquad \boldsymbol{F}_{\mathrm{i}}^{\mathrm{n+1}} = \boldsymbol{F}_i^n + \left(\frac{\partial \boldsymbol{F}}{\partial \boldsymbol{U}}\right)_i^n \left(\boldsymbol{U}_i^{n+1} - \boldsymbol{U}_{\mathbf{i}}^{\mathbf{n}}\right). \tag{18}$$

where the Jacobian matrices for the derivation of the source term and flux vectors with regard to the state vector $\boldsymbol{U}$ have been algebraically evaluated in order to save computational time. The final solution for the new-time conservative parameters is done by a Newton-Raphson iteration. Experience shows that convergence is achieved within less than 2 to 3 iteration steps. The fully implicit time integration allows the use of larger time steps and, therefore, significantly reduces the necessary computing time which is of particular interest for more complex problems.

The numerical method applied and briefly summarized above provides considerably reduced numerical diffusion and/or viscosity effects compared with standard finite difference methods based on staggered grids and donor cell techniques. This is of particular importance if strong parameter gradients exist in the flow (e.g. two-phase mixture levels) or in general for multi-dimensional flow processes governed by (physical) viscous drag forces. More details to the numerical solution method are given in [21, 22].

6 NUMERICAL EXAMPLES

The two-phase modelling and numerical solution technique described in section 5 is the basis for the JRC **Advanced Two-phase Flow Module** (ATFM) which has been specifically developed to assess new computational strategies for the numerical solution of multi-dimensional transient two-phase flows. A large number of physical and numerical benchmark test cases have been performed to verify the predictive capability of the models and numerical techniques; selected results of which can be found in [21] to [23]. In the following only a few results are shown which are of interest for future nuclear safety applications.

6.1 Edwards' Pipe Blowdown with Downstream Jet Formation

A standard test case for TH codes has been the blowdown of an initially hot pressurized liquid from a pipe of approximately 4 m length, also known as CSNI standard problem No. 1 (Edwards' pipe) [24]. The water in the pipe has an initial pressure of 7.0 MPa and a temperature of 502 K which corresponds to an initial subcooling of 56.8 K. The transient is initiated by the rupture of a bursting disk allowing the rapid discharge to the environment at atmospheric pressure.

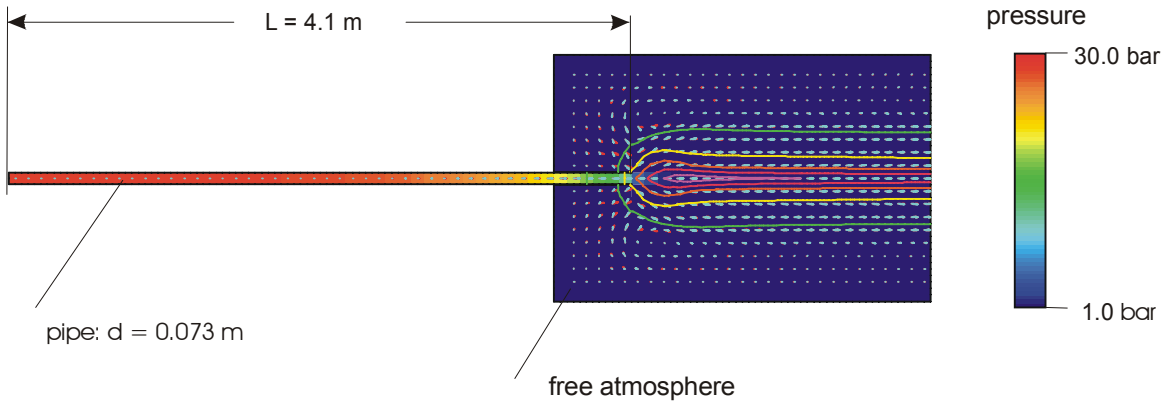

Figure 5: Pressure distribution and iso-Mach lines at t = 0.02 s after break

In order to avoid the specification of boundary condition at the very sensitive area at the pipe exit, a further expansion of the two-phase mixture and jet formation downstream of the pipe is modelled as a quasi (axisymmetric) three-dimensional flow process with a constant (atmospheric) far-field pressure boundary. Predicted pressure field and corresponding iso-Mach lines at 0.02 s after the break of the rupture disk are shown in Fig. 5.

The first 10 ms of the transient are characterized by the propagation of a rarefaction wave from the opening back into the pipe and the reflection of the wave at the closed end of the pipe where a distinct undershoot of the pressure occurs.

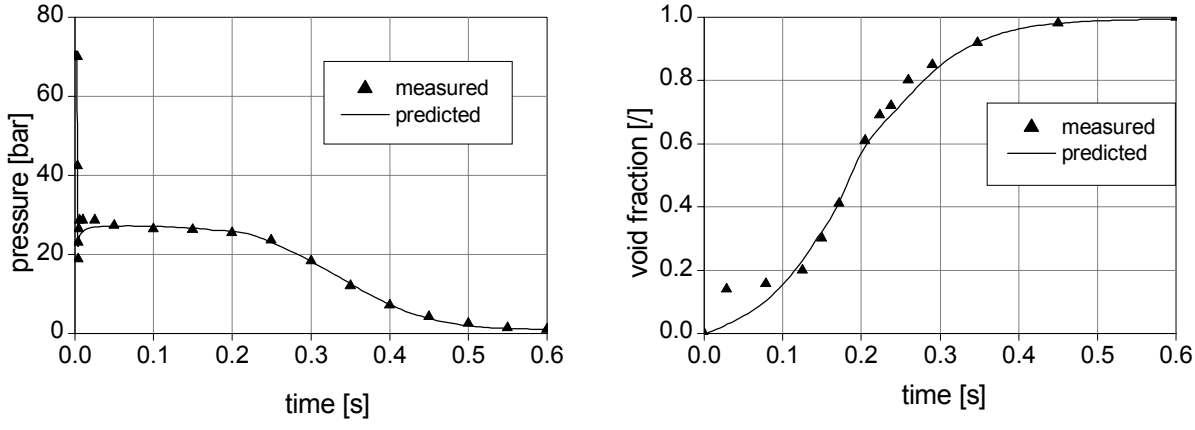

Figure 6 : Pressure at pipe head and void fraction at pipe middle section

After this first pressure wave propagation period, an evaporation front moves into the pipe and, with the onset of bulk evaporation, the blowdown is controlled by the two-phase discharge from the pipe, the continuous evaporation (flashing) of liquid as well as the frictional forces at the pipe walls. As an example, measured and predicted values for the pressure at the pipe head and the void fraction at the pipe middle section are shown in Fig. 6.

The good agreement between measured and predicted data suggests that the governing phenomena of the blowdown process are correctly predicted.

6.2 ROSA-I Vessel Blowdown Tests

In the ROSA-I test programme a series of blowdown experiments were performed to study the thermal-hydraulic phenomena associated with a Loss-of-Coolant Accident (LOCA) in Pressurized Water Reactors [25]. The experiments were carried out by discharging initially saturated water at high pressure from a vessel of 1.9 m^3 volume. The discharge points were located at the top and the bottom of the vessel. The transient was initiated by a rupture disk installed at the end of a short stand-pipe. The break size was varied by means of orifices of different diameter.

For data comparison, a top venting test has been selected with an initial pressure of 70 bar and break sizes of 50 and 70 mm. The transient is governed by a fast depressurization in the liquid pool, level swell with strong multi-dimensional flow phenomena and temporary water hold-up in the upper vessel region. During the latter stages of the transient, gravity induced phase separation becomes dominant resulting in the collapsing of any remaining liquid and the formation of a residual water pool. The prediction was made in a three-dimensional manner with a hexagonal grid of 500 cells.

All the phenomena as mentioned above are well represented in the calculation as shown in Fig. 7 for a top-venting case with 70 mm orifice. Measured and predicted values for the pressure in the vessel and the mass inventory during the transient are compared in Fig. 8 for two different break sizes.

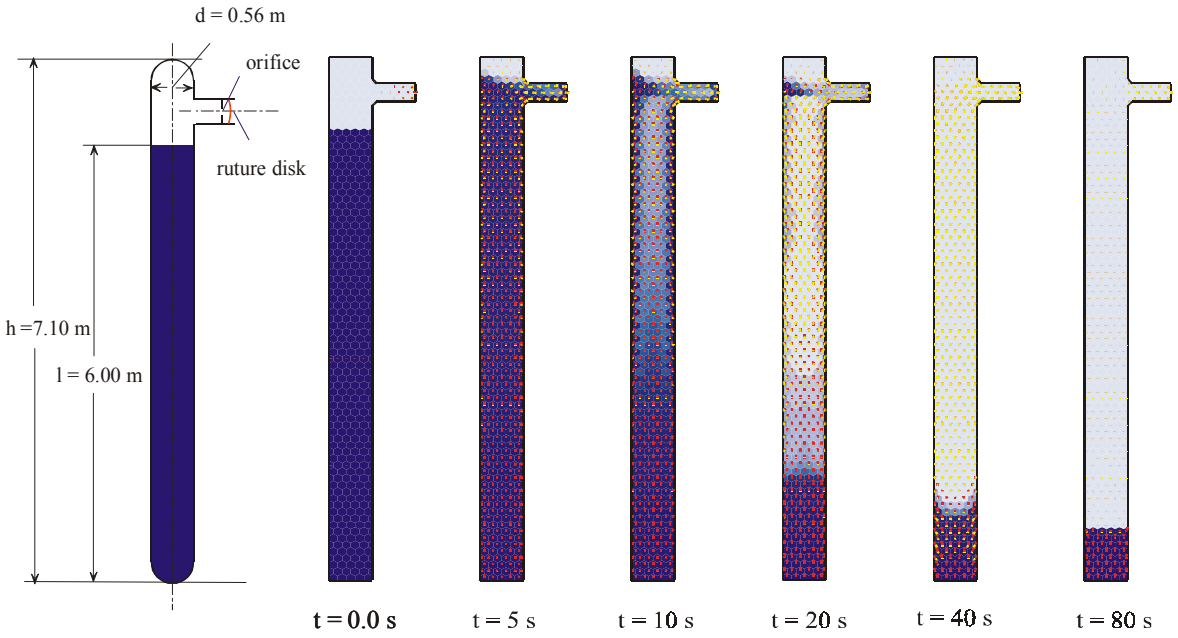

Figure 7: ROSA-I vessel blowdown, predicted void fraction and flow vector fields at different time values.

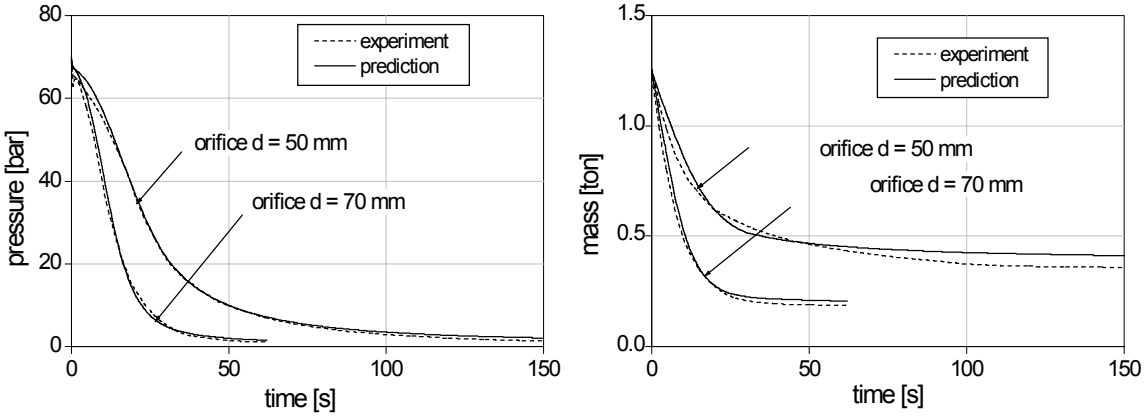

Figure 8: ROSA-I vessel blowdown, comparison of measured and predicted pressure and mass inventory for two different break sizes

7 SUMMARY

Although present best-estimate TH-codes have reached a high degree of maturity, there still remain shortcomings in the codes which are often related to limitations of the basic modelling approach or the numerical methods applied. There is also some evidence that most codes have reached a level of developmental "saturation". This is indicated by the observation that further code improvement programmes had only marginally improved the quality of the prediction as long as the underlying basic physical modelling concept and numerical method applied are maintained. On the other hand, more fundamental changes to the modelling like the use of multi-field equations, interfacial area transport models, or the use of new low-diffusive numerical methods can hardly be realized in the framework of the present code structures.

The future perspective for TH-codes will largely depend on the time frame considered. Although the present TH-codes no longer represent the "state-of-the-art" in many aspects, they will certainly continue (at least in a short term view) to play an important role for the safety assessment of LWRs with standard or evolutionary designs. Major efforts in the near term might concentrate on making them easier to use and on quantifying uncertainties associated with the predictions.

As suggested in the present paper, there are various promising new concepts with respect to the physical modelling, numerical method and informatics which could justify a new attempt for the development of a “third generation” of TH-codes. On a long term view, such a project might be the only way to maintain the (still) existing large competences in reactor thermal hydraulics and in related fields like transient two-phase flow and boiling heat transfer or neutron kinetics. However, the final decision on this subject will certainly be driven by the future needs in this field coming from the nuclear industry or public authorities.

REFERENCES

[1] M. Ishii, *Thermodynamics of Two-Phase Flow*, Eyrolles, Paris, 1975

[2] A. Boure, *On a Unified Presentation of the Non-Equilibrium Two-Phase Flow Models*, Proc. of ASME Symp., New York, 1975.

[3] J. M. Delhaye, J. L. Achard, *On the Averaging Operators Introduced in Two-Phase Flow Modelling* , Proc.CSNI Specialist Mtg. on Transient Two-Phase Flow, Toronto, 1976.

[4] D. Drew, R.T Lahey, *Application of General Constitutive Principles to the Derivation of the Multidimensional Two-phase Flow Equations*, Int. J. Multiphase Flow, Vol.5, p 243-

[5] D. Drew, I. Cheng, R. T. Lahey, *The Analysis of Virtual Mass Effects in Two-phase Flow*, Int. J.Multiphase Flow 5, No. 4, 233-242, 1979.

[6] D. Gidaspow (chairman), *Modelling of Two-Phase Flow*, Round Table Discussion RT-1-2, proceedings of the Fifth International Heat Transfer Conference, Tokyo, Japan, September 3-7, 1974, also in Heat Transfer, 3 (1974)

[7] *RELAP5/MOD3 Code Manual, Volume I : Code Structure, System Models and Solution Methods*, NUREG/CR-5535, 1995

[8] *TRAC-M/FORTRAN90, Theory Manual*, NUREG/CR-6724, July 2001

[9] F. H. Harlow, A.A. Amsden*, A Numerical Fluid Dynamics Calculation Method for all Speeds*, Journal of Computational Physics, 8, (1971), 197-213

[10] F. H. Harlow, A.A. Amsden, *Numerical Calculation of Multiphase Flow*, Journal of Computational Physics, 17, (1975), 19-52

[11] J.H. Mahaffy, *A Stability Enhancing Two-step Method for Fluid Flow*, Los Alamos Scientific Laboratory Report, LA-7951-MS, US Nuclear Regulatory Commission, NUREG/CR-0971 (1979)

[12] J.H. Mahaffy, *A Stability Enhancing Two-step Method for Fluid Flow Calculations*, J. Computational Physics 8, pp 197-213, 1871)

[13] D. Bestion, *Module de Base de CATHARE, Equations du Module Axial, Analyse Numerique du Module Axial*, SETh/LEML-EM/89-157, CEA Grenoble

[14] M. Burwelll, G. Lerchel, G. Miro, V. Teschendorff, K. Wolfert, *The Thermal-Hydraulic Code ATHLET for Analysis of PWR and BWR Systems*, Proc. 4th Intern. Topical Meeting on Nuclear Reactor Thermal-Hydraulics, NURETH-4, Karlsruhe, Vol.2, pp. 1093-1102, 1988

[15] I. Tuomi, F. Barre, H. Städtke, U. Graf, S. Mimouni, *Advances in Numerical Methods f or Two-phase Flows,* OECD/CSNI Workshop on Advanced Thermal-hydraulic and Neutronic Codes, April 12-14, 200, Barcelona, Spain

[16] H. Städtke, R. Holtbecker*, Hyperbolic Model for Inhomogeneous Two-Phase Flow*, Intern. Conference on Multiphase Flows, '91 TSUKUBA, Univ. of Tsukuba, Japan, September 24-27, 1991

[17] H. Städtke, B. Worth, *On the Hyperbolic Nature of Two-phase Flow Equations, Characteristic Analysis and Related Numerical Methods,* Intern. Conference on Godunov Methods, Theory and Applications, October 1999, Oxford, UK, to be published by Kluwer-Academic/Plenum Publisher

[18] G. Kocamustafaogullari, M. Ishii, *Foundation of the Interfacial Area Transport Equations and its Closure Relations*, Int. J. Heat and Mass transfer, Vol. 38, N0. 3, pp. 481-493, 1995

[19] H. Städtke, A. Blahak, B. Worth, *Modelling of Interfacial Area Concentration in Two-Phase Flow Systems*, 8th Intern. Meeting on Nuclear Thermal Hydraulics, Kyoto, Japan, September30 - October 4, 1997

[20] B. Van Leer, *Towards the Ultimate Conservative Difference Scheme, Second order Sequel to Godunov's Method*, J. Computational Phys. 32, 1979

[21] H. Städtke, G. Franchello and B. Worth, *Numerical Simulation of Gas-Liquid Flows Using Second Order Flux Splitting Techniques,* 8th Int. Conference on Computational Fluid Dynamics

[22] H. Städtke, G. Franchello and B. Worth, *Numerical Simulation of Two-phase Flows with Stiff Source Terms,* First. Intern. Conference on Computational Fluid Dynamics, July 9-14, 2000, Kyoto, Japan

[23] H. Städtke and G. Franchello, B. Worth, *Characteristic based Upwind method for Two-phase Flow, Present Status and Future Perspective,* paper accepted for Intern. Conference on Multiphase Flow, ICMF 2001, Louisiana, USA

[24] A.R. Edwards, T.P. O'Brien, *Studies of Phenomena Connected with the Depressurization of Water Reactors*, J. Br. Nucl. Energy 9, 1970, pp 125-135

[25] M. Sobajima, *An Analysis of Transients in Experiments on Loss-of-Coolant Accidents,* Nuclear Science and Engineering, 60, 10-18, 1976